

Structural and Functional Models of the Dioxygen-Activating Centers of Non-Heme Diiron Enzymes Ribonucleotide Reductase and Soluble Methane Monooxygenase

Dongwhan Lee and Stephen J. Lippard*

Department of Chemistry
Massachusetts Institute of Technology
Cambridge, Massachusetts 02139

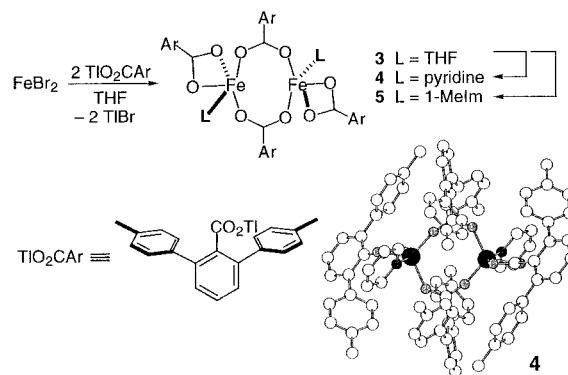
Received August 31, 1998

The carboxylate-bridged non-heme diiron centers in the R2 protein of ribonucleotide reductase (RNR-R2) and the hydroxylase component of soluble methane monooxygenase (MMOH) activate dioxygen to produce a functional tyrosyl radical and to convert methane to methanol, respectively.^{1–4} A structurally analogous diiron unit has also been identified in Δ^9 stearyl-acyl carrier protein desaturase (Δ^9 D), an enzyme that introduces a cis double bond into a saturated fatty acid substrate.⁵ To date no accurate structural and functional model of these centers has been reported.^{6,7} In the present paper we describe the use of a sterically hindered carboxylate that has enabled us to access coordinatively unsaturated carboxylate-bridged diiron(II) complexes that are geometrically analogous to those of the reduced RNR-R2,⁸ MMOH,⁹ and Δ^9 D⁵ enzyme active sites. Moreover, reaction of these complexes with dioxygen in CH_2Cl_2 afforded metastable green species that convert nearly quantitatively into a compound having the unprecedented *trans,trans*-bis(μ -hydroxo)bis(μ -carboxylato)diiron(III) core. Addition of 2,4,6-*tert*-butylphenol to the colored intermediates generated the phenoxyl radical, chemistry analogous to that observed in RNR-R2.

In an effort to find carboxylate ligands capable of forming kinetically stable dinuclear iron complexes, we investigated sterically hindered carboxylic acids derived from *m*-terphenyl. In particular, molecular modeling suggested that 2,6-di(*p*-tolyl)benzoate (**1**)^{10–12} might facilitate formation of the desired bis(μ -carboxylato)diiron(II) core. The introduction of *p*-tolyl groups at the 2- and 6-positions of the bridging benzoate not only provides a hydrophobic cavity in the vicinity of the dimetallic center but also serves effectively to shield against undesired bimolecular decomposition pathways which typically occur in reactions of dioxygen with diiron(II) complexes.^{13,14}

A neutral bis(μ -carboxylato)diiron(II) complex, $[\text{Fe}_2(\mu\text{-O}_2\text{CAR})_2(\text{O}_2\text{CAR})_2(\text{THF})_2]$ (**3**), was prepared by reaction of 1.84 mmol of

Scheme 1



FeBr_2 with 2 equiv of TlO_2CAR (**2**) in 45 mL of THF (Scheme 1). Compound **3** served as a convenient starting material for subsequent ligand exchange reactions. When a CH_2Cl_2 solution of **3** was treated with 2.2 equiv of pyridine, $[\text{Fe}_2(\mu\text{-O}_2\text{CAR})_2(\text{O}_2\text{CAR})_2(\text{py})_2]$ (**4**) was obtained in 75% yield after recrystallization. As illustrated in Figure 1, the diiron(II) core in **4** is composed of two five-coordinate iron atoms related by a crystallographic inversion center. These atoms are bridged by two carboxylates which coordinate in an unsymmetrical *syn, syn*-bidentate¹⁵ mode. The remaining coordination sites are filled by two terminal chelating carboxylates and by two pyridine ligands. The geometry of the resulting iron centers is best described as highly distorted trigonal bipyramidal. The $\{\text{Fe}_2(\mu\text{-O}_2\text{CAR})_2(\text{O}_2\text{CAR})_2\}$ core structure of **4** is nearly congruent with that of **3**, in which the $\text{Fe}\cdots\text{Fe}$ distance is 4.2822(7) Å. The zero-field Mössbauer spectra obtained at 77 K for **3** and **4** are also quite similar. Both the isomer shifts, $\delta = 1.24$ mm/s for **3** and 1.17 mm/s for **4**, and quadrupole splitting parameters, $\Delta E_Q = 2.85$ mm/s for **3** and 2.98 mm/s for **4**, are characteristic of high-spin iron(II) species. When **3** was allowed to react with 1-methylimidazole (1-MeIm) instead of pyridine, the structurally analogous diiron(II) complex $[\text{Fe}_2(\mu\text{-O}_2\text{CAR})_2(\text{O}_2\text{CAR})_2(1\text{-MeIm})_2]$ (**5**) was obtained. Recrystallization from CH_2Cl_2 /pentane afforded crystals for an X-ray structure analysis which revealed two different coordination modes for the terminal carboxylate ligands. In one of two molecules of **5** in the asymmetric unit, these ligands have undergone carboxylate shifts from the chelating geometry observed in the analogous complex **4** to monodentate terminal coordination. The resulting structure contains two four-coordinate iron(II) centers and nearly reproduces the geometry of the reduced RNR-R2 and MMOH cores.^{8,9} The only difference is the relative positioning of the N-donor ligands, which are anti in the model compound and *syn* in the proteins. The other molecule in the asymmetric unit of **5** has chelating terminal carboxylate ligands, retaining the two five-coordinate centers found in **4** and in Δ^9 D.⁵

Although the $\{\text{Fe}_2(\mu\text{-O}_2\text{CAR})_2(\text{O}_2\text{CAR})_2\}$ core structure is retained in both **3** and **4**, the change from THF to pyridine terminal ligands significantly alters their reactivity with dioxygen. At -78°C , introduction of O_2 into a CH_2Cl_2 solution of **3** immediately affords a yellow color. Under the same conditions, however, **4** converts to a deep emerald green species that is stable for >6 h, but the solution turns yellow upon warming. From this reaction, the quadruply bridged diiron(III) complex $[\text{Fe}_2(\mu\text{-OH})_2(\mu\text{-O}_2\text{CAR})_2(\text{O}_2\text{CAR})_2(\text{py})_2]$ (**6**) was obtained in nearly quantitative ($>90\%$) yield after recrystallization.

Compound **6** represents the first structurally characterized example of a bis(μ -hydroxo)bis(μ -carboxylato)dimetallic unit and

- (1) Feig, A. L.; Lippard, S. J. *Chem. Rev.* **1994**, *94*, 759–805.
- (2) Valentine, A. M.; Lippard, S. J. *J. Chem. Soc., Dalton Trans.* **1997**, 3925–3931.
- (3) Wallar, B. J.; Lipscomb, J. D. *Chem. Rev.* **1996**, *96*, 2625–2657.
- (4) Stubbe, J.; van der Donk, W. A. *Chem. Rev.* **1998**, *98*, 705–762.
- (5) Lindqvist, Y.; Huang, W.; Schneider, G.; Shanklin, J. *EMBO J.* **1996**, *15*, 4081–4092.
- (6) Que, L., Jr.; Dong, Y. *Acc. Chem. Res.* **1996**, *29*, 190–196.
- (7) Que, L., Jr. *J. Chem. Soc., Dalton Trans.* **1997**, 3933–3940.
- (8) Logan, D. T.; Su, X.-D.; Aberg, A.; Regnström, K.; Hajdu, J.; Eklund, H.; Nordlund, P. *Structure* **1996**, *4*, 1053–1064.
- (9) Rosenzweig, A. C.; Nordlund, P.; Takahara, P. M.; Frederick, C. A.; Lippard, S. J. *Chem. Biol.* **1995**, *2*, 409–418. Recently, a second crystal form of MMOH has been obtained, (Rosenzweig, A. C.; Brandstetter, H.; Whittington, D. A.; Nordlund, P.; Lippard, S. J.; Frederick, C. A. *Proteins* **1997**, *19*, 141–152), which, upon reduction in the crystal, affords a diiron(II) center with two bidentate glutamate ligands such as those in reduced RNR-R2 (Whittington, D. A.; Lippard, S. J., unpublished results).
- (10) Du, C.-J. F.; Hart, H.; Ng, K.-K. D. *J. Org. Chem.* **1986**, *51*, 3162–3165.
- (11) Chen, C.-T.; Siegel, J. S. *J. Am. Chem. Soc.* **1994**, *116*, 5959–5960.
- (12) Saednya, A.; Hart, H. *Synthesis* **1996**, 1455–1458.
- (13) Feig, A. L.; Becker, M.; Schindler, S.; van Eldik, R.; Lippard, S. J. *Inorg. Chem.* **1996**, *35*, 2590–2601.
- (14) Feig, A. L.; Masschelein, A.; Bakac, A.; Lippard, S. J. *J. Am. Chem. Soc.* **1997**, *119*, 334–342.

- (15) Rardin, R. L.; Tolman, W. B.; Lippard, S. J. *New J. Chem.* **1991**, *15*, 417–430.

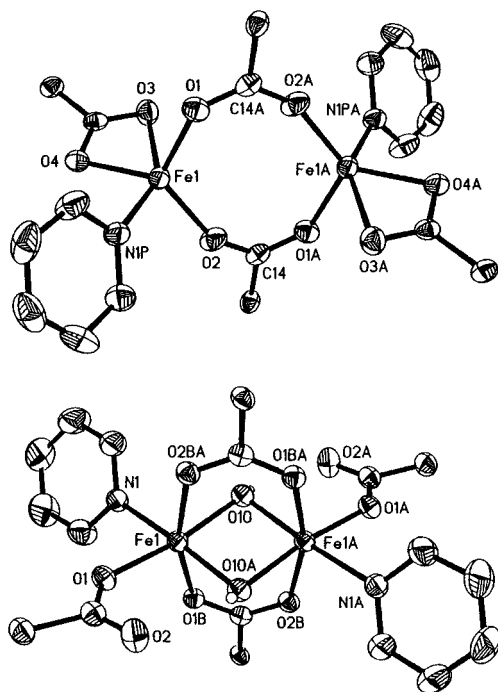


Figure 1. ORTEP diagram of $[\text{Fe}_2(\mu\text{-O}_2\text{CAR})_2(\text{O}_2\text{CAR})_2(\text{py})_2]$ (**4**) (top) and $[\text{Fe}_2(\mu\text{-OH})_2(\mu\text{-O}_2\text{CAR})_2(\text{O}_2\text{CAR})_2(\text{py})_2]$ (**6**) (bottom, one of two molecules in the asymmetric unit) showing 50% probability thermal ellipsoids for non-hydrogen atoms. For clarity, all atoms of the 2,6-di-(*p*-tolyl)benzoate ligands, except for the carboxylate groups and the α -carbon atoms, were omitted. Selected interatomic distances (\AA) and angles (deg): (top) $\text{Fe1}\cdots\text{Fe1A}$, 4.2189(13); Fe1-O1 , 2.006(3); Fe1-O2 , 1.957(3); Fe1-O3 , 2.358(3); Fe1-O4 , 2.047(3); Fe1-N1P , 2.132(4); Fe1-O1-C14A , 135.6(3); Fe1A-O2A-C14A , 152.8(3); O3-Fe1-O4 , 59.18(11); O1-Fe1-O2 , 116.42(13); N1P-Fe1-O1 , 98.65(13); N1P-Fe1-O2 , 96.26(13); N1P-Fe1-O4 , 90.01(13); N1P-Fe1-O3 , 148.25(13). (bottom) $\text{Fe1}\cdots\text{Fe1A}$, 2.8843(9); Fe1-O10 , 2.012(2); Fe1-O10A , 1.986(2); Fe1-O1B , 2.040(2); Fe1-O2BA , 2.076(2); Fe1-O1 , 1.969(2); Fe1-N1 , 2.149(3); $\text{O2}\cdots\text{O10A}$, 2.888(3); Fe1-O10-Fe1A , 92.33(10); O10-Fe1-O10A , 87.66(10).

provides in a discrete dinuclear complex a carboxylate-bridged bis(μ -hydroxo)diiron(III) fragment similar to that present in oxidized MMOH (Figure 1). The $\text{Fe}\cdots\text{Fe}$ distances of 2.8472(8) and 2.8843(9) \AA for the two chemically equivalent molecules of **6** in the crystallographic asymmetric unit are substantially shorter than those in the precursor **4** owing to the presence of the two bridging OH^- groups. These units were unambiguously assigned as hydroxide ions by the Fe-O bond distances ranging from 1.969(3) to 2.012(2) \AA and by the location and refinement of the hydrogen atoms in the X-ray crystal structure determination. The two bridging carboxylate groups in **6** are disposed trans to one another across the $\{\text{Fe}_2(\text{OH})_2\}^{4+}$ plane, and the two terminal carboxylate ligands are hydrogen-bonded to the bridging hydroxo ligands ($\text{O2}\cdots\text{H-O10A}$, 2.888(3) \AA). In contrast to the relatively small difference in intermetallic distance between doubly bridged bis(μ -hydroxo)diiron(III) (3.078–3.155 \AA)^{16–18} and triply bridged bis(μ -hydroxo)(μ -carboxylato)diiron(III) (3.042 \AA)¹⁹ cores, the $\text{Fe}\cdots\text{Fe}$ distance shortens significantly (see above) upon addition of a fourth, carboxylate, bridge. The short

$\text{Fe}\cdots\text{Fe}$ distance (2.46 \AA) derived from an EXAFS analysis of intermediate **Q**,²⁵ and the recent discovery of two *syn,syn*-bridging carboxylate residues in the X-ray structure of reduced form II crystals of MMOH from *Methylococcus capsulatus* (Bath),⁹ suggest that similar quadruply bridged species may occur in the MMOH reaction cycle.

At present we do not know exactly how **4** converts to **6** upon addition of dioxygen. Formal reduction of O_2 to two OH^- ions would be a four-electron process. If two electrons come from iron, the other two might arise from hydrogen atoms. One source of the latter could be the methyl groups on the carboxylate ligands, but we can rule out that possibility from the high yield of the reaction and our ability to extract the ligand from the thermolysis reaction mixture and establish its integrity by ^1H NMR spectroscopy and mass spectrometry. Oxidation of **4** to the diiron(III) level followed by hydroxide addition from adventitious water could also account for the formation of **6**. This oxidation chemistry inspired us to investigate the reaction of the deep green metastable species formed by oxygenation of **4** at -78°C with 2,4,6-tri-*tert*-butylphenol, an analogue of the tyrosine residue present at the active site of the RNR-R2 enzyme. The result was the formation of the corresponding phenoxy radical, as demonstrated both by UV/vis ($\lambda_{\text{max}} = 383, 401 \text{ nm}$) and EPR ($g = 2.0045$ at 77 K) spectroscopy. Although the details of the formal O-H bond homolysis in this reaction have not yet been elucidated, it provides the first example where the oxidation chemistry of RNR-R2 has been successfully mimicked with a synthetic structural analogue.²⁶

In summary, novel bis(μ -carboxylato)diiron(II) complexes have been assembled which reproduce many features of the catalytic centers in carboxylate-bridged non-heme diiron proteins. The mechanism of formation of the quadruply bridged diiron(III) complex, as well as the structures of metastable species involved in the pathway, are currently under investigation.

Acknowledgment. This work was supported by grants from the National Science Foundation, National Institute of General Medical Sciences and AKZO. We thank Professor W. M. Reiff of Northeastern University for access to Mössbauer equipment and Drs. J. Du Bois, P. Fuhrmann, and T. J. Mizoguchi for helpful discussions.

Supporting Information Available: Details of the synthetic procedures, X-ray crystallographic tables, and physical characterization of **2–6** as well as spectral characterization of the oxygenation reaction products (63 pages, print/PDF). See any current masthead page for ordering and Internet access instructions. An X-ray crystallographic file, in CIF format, is available through the Web only. See any current masthead page for ordering information and Web access instructions.

JA9831094

(19) A discrete bis(μ -hydroxo)(μ -carboxylato)diiron(III) unit, the core structure present at the active site of MMOH_{ox}, has yet to be achieved in inorganic chemistry. $\text{Fe}\cdots\text{Fe}$ separations of 3.010–3.035 \AA ^{20–23} occur in "molecular ferric wheel" clusters containing bis(μ -methoxo)(μ -carboxylato)diiron(III) cores. A comparable $\text{Fe}\cdots\text{Fe}$ distance (3.042 \AA) was recently observed in the bis(μ -hydroxo)(μ -carboxylato)diiron(III) core of a hexairon cluster.²⁴

(20) Taft, K. L.; Lippard, S. J. *J. Am. Chem. Soc.* **1990**, *112*, 9629–9630.
(21) Taft, K. L.; Delfs, C. D.; Papaefthymiou, G. C.; Foner, S.; Gatteschi, D.; Lippard, S. J. *J. Am. Chem. Soc.* **1994**, *116*, 823–832.

(22) Benelli, C.; Parsons, S.; Solan, G. A.; Wimpenny, R. E. P. *Angew. Chem., Int. Ed. Engl.* **1996**, *35*, 1825–1828.

(23) Watton, S. P.; Fuhrmann, P.; Pence, L. E.; Caneschi, A.; Cornia, A.; Abbati, G. L.; Lippard, S. J. *Angew. Chem., Int. Ed. Engl.* **1997**, *36*, 6, 2774–2776.

(24) Lee, D.; Lippard, S. J., unpublished results.

(25) Shu, L.; Nesheim, J. C.; Kauffmann, K.; Münck, E.; Lipscomb, J. D.; Que, L., Jr. *Science* **1997**, *275*, 515–518.

(26) Oxidation of a substituted phenol to its phenoxy radical has also been effected by (μ -peroxo)diiron(III)²⁷ or bis(μ -oxo)iron(III)iron(IV)²⁸ species.

(27) Dong, Y.; Ménage, S.; Brennan, B. A.; Elgren, T. E.; Jang, H. G.; Pearce, L. L.; Que, L., Jr. *J. Am. Chem. Soc.* **1993**, *115*, 1851–1859.

(28) Kim, C.; Dong, Y.; Que, L., Jr. *J. Am. Chem. Soc.* **1997**, *119*, 3635–3636.

(16) Thich, J. A.; Ou, C. C.; Powers, D.; Vasiliou, B.; Mastropaolo, D.; Potenza, J. A.; Schugar, H. J. *J. Am. Chem. Soc.* **1976**, *98*, 1425–1433.

(17) Ou, C. C.; Lalancette, R. A.; Potenza, J. A.; Schugar, H. J. *J. Am. Chem. Soc.* **1978**, *100*, 2053–2057.

(18) Borer, L.; Thalken, L.; Ceccarelli, C.; Glick, M.; Zhang, J. H.; Reiff, W. M. *Inorg. Chem.* **1983**, *22*, 1719–1724.